Doping of $GaN_{1-x}As_x$ with High As content

A. X. Levander[1,2], S. V. Novikov[3], Z. Liliental-Weber[1], R. dos Reis[1,4], O. D. Dubon[1,2], J. Wu[1,2], C. T. Foxon[3], K. M. Yu[1], and W.Walukiewicz[1]

[1] *Materials Sciences Division, Lawrence Berkeley National Laboratory, Berkeley, CA 94720 USA*
[2] *Department of Materials Science & Engineering, University of California, Berkeley, CA 94720*
[3] *School of Physics and Astronomy, University of Nottingham, Nottingham NG7 2RD, UK*
[4] *Instituto de Física, UFRGS, Porto Alegre, RS 15051, 91501-970 Brazil*

Recent work has shown that $GaN_{1-x}As_x$ can be grown across the entire composition range by low temperature molecular beam epitaxy with intermediate compositions being amorphous, but control of the electrical properties through doping is critical for functionalizing this material. Here we report the bipolar doping of $GaN_{1-x}As_x$ with high As content to conductivities above 4 S/cm at room temperature using Mg or Te. The carrier type was confirmed by thermopower measurements. Doping requires an increase in Ga flux during growth resulting in a mixed phase material of polycrystalline GaAs:N embedded in amorphous $GaN_{1-x}As_x$.

Electronic mail: kmyu@lbl.gov

I. INTRODUCTION

The key advance in amorphous silicon (a-Si) leading to its applications in thin film electronics and photovoltaics was the ability to dope the material both *p*-type and *n*-type[1-3]. a-Si photovoltaic technology has since advanced by taking advantage of a range of band gaps accessible through alloying with germanium or carbon[4,5]. Alloying of a-Si has led to multi-junction solar cells with somewhat higher efficiencies, but it also causes reduced electrical performance due to higher defect densities[6,7]. The poor conductivity and the limited bandgap range of a-Si alloys severely hinder the widespread applications of a-Si alloys despite their potential advantages of lower cost and ability to deposit on flexible substrates. To overcome these deficiencies, amorphous compound semiconductors such as a-GaAs grown either by sputtering or plasma-enhanced chemical vapor deposition have been explored[8,9]. However, the inability to dope these compound semiconductors, explained theoretically by a self-compensation mechanism, reduced the interest in amorphous compound semiconductors[10,11]. In this paper, we report the demonstration of *p*-type and *n*-type doping of a partially amorphous III-V compound semiconductor alloy $GaN_{1-x}As_x$ to room temperature conductivities as high as 4.8 S/cm, higher than typical conductivities for hydrogenated a-Si in the range of $10^{-2} – 10^{-1}$ S/cm[8, 12]. The ability to control the electrical properties of these alloys that exhibit a wide bandgap range of 0.8-3.4 eV can lead to exciting applications in electronics and photovoltaics.

Crystalline $GaN_{1-x}As_x$ in the As-rich or N-rich regimes has been extensively studied as a so-called highly mismatched alloy (HMA) due to the dramatic restructuring

of the electronic bands caused by the isoelectronic substitution of the anion with another of very different electronegativity and/or atomic radius[13-16]. Recently we have reported success in growing $GaN_{1-x}As_x$ across the entire composition range using highly non-equilibrium low-temperature molecular beam epitaxy (LT-MBE)[17,18]. Although the resulting alloys are amorphous in the intermediate composition range ($0.10 < x < 0.75$), the band gap continues to change monotonically with alloy concentration, in agreement with the band anticrossing model for HMAs[19]. *Ab initio* molecular dynamics calculations for amorphous GaN have suggested that the highly electronegative nitrogen may result in a lower density of mid-gap states[20]. High densities of mid-gap states have a tendency to pin the Fermi energy, preventing control over the electrical properties. The lower density of mid-gap states in nitride based amorphous semiconductors may facilitate the doping of a-$GaN_{1-x}As_x$.

Due to the low growth temperature of 200-320°C and the amorphous structure, these $GaN_{1-x}As_x$ films can be grown on low cost glass substrates instead of expensive single crystal substrates[19]. The amorphous nature of these alloys has the added advantage of material flexibility and hence the potential for applications on plastic substrates. Despite the highly non-equilibrium composition of these alloys, they are remarkably stable for short excursions beyond 700°C prior to phase segregation[21]. The thermal stability of these alloys is important for functionalization due to various high temperature semiconductor processing techniques (e.g. dielectric deposition). However, all the potential applications of these alloys critically depend on the availability to dope them *p*- and *n*-type.

II. EXPERIMENTAL

In this work, the $GaN_{1-x}As_x$ thin films were grown by plasma-assisted molecular beam epitaxy on c-plane sapphire at temperatures between 200-320°C. Typical beam equivalent pressures (BEPs) for homogeneously amorphous material are 1.5×10^{-5} Torr for N, 7.7×10^{-6} Torr for As, and 1.1×10^{-7} Torr for Ga. Further details of the growth are described in Refs. 17-18. For *p*-type doping, the Mg content in the film was controlled by the Mg BEP. The composition and thickness of the alloy and the total amount of Mg incorporated in the films was determined by Rutherford backscattering spectrometry (RBS) with a 3.04 MeV He^{2+} beam to simultaneously examine the films for oxygen contamination taking advantage of the $^{16}O(\alpha,\alpha)^{16}O$ resonance reaction. Due to the uncertainty in the bonding configuration of the dopants in the disordered structure, the atomic percentage of the dopant is reported. The composition and thickness of $GaN_{1-x}As_x$ films reported here are x~0.55-0.65 and ~ 1 μm, respectively. The $GaN_{1-x}As_x$:Mg/Te films are stoichiometric with a (III+II)/(V+VI) atomic ratio of unity +/- 3%. The absorption onset characterized by UV-Vis spectroscopy is near 1 eV, in agreement with our previous work[17,18].

III. RESULTS AND DISCUSSION

Electrical conductivity measurements were conducted in the Van der Pauw geometry using a liquid helium cryostat using pressed indium contacts made after a brief HCl dip. The ohmic behavior of the contacts was verified by the linear behavior of the

current-voltage curve. The result of the Mg incorporation on the direct-current conductivity of a series of $GaN_{0.35}As_{0.65}$ films is shown in Fig. 1. The conductivity increased monotonically with increasing magnesium content, up to a maximum value of 4.86 S/cm at room temperature for 8 at% Mg. The low temperature region (50-6K) of the Arrhenius plot of $ln(\sigma)$ versus 1/T remains linear and from this an activation energy (E_a) for the conduction was determined (Fig. 1 inset). With increased magnesium doping, the E_a decreased from 215 meV to 0.32 meV.

Ionization energies for acceptors in GaAs and GaN are in the range of 10-100s meV so the low energy thermally activated transport provides a clear evidence for the hopping conduction, indicating the presence of large local fluctuation of the valence band edge[22]. The reduction of E_a with increasing Mg content can be attributed to an increase in the hole concentration and associated moving of the Fermi energy, E_f, toward the valence band. At low concentrations the holes are localized in isolated low energy valleys and the transport is determined by the thermal activation over energy barriers. The effective barrier height decreases as E_f moves deeper into the valence band and for high enough hole concentrations the holes regain their extended character and the material shows nearly metallic, weakly temperature dependent conductivity. According to Hall measurements performed in a 7 Tesla field, the room temperature Hall mobility of the sample with 1% Mg was approximately 1 cm^2/Vsec with a carrier concentration of ~1×10^{17} cm^{-3}. The sample with the highest conductivity had a Hall mobility of approximately 0.3 cm^2 /Vsec with a carrier concentration of ~1×10^{20} cm^{-3}. The low mobility is attributed to the disordered structure and indicates a strong alloy disorder scattering in this HMA. Although the hole concentration is high, it is still much lower

than the concentration of Mg atoms. However, such low doping efficiency is typical of amorphous semiconductor materials, where, e.g., up to 1 at% of phosphorous or boron is required for achieving good conductivity in a-Si[1,23].

In order to confirm that magnesium was indeed behaving as an acceptor, donating holes to the valence band, the thermopower was measured for both doped and undoped films. Thermopower measurements were conducted using a home-built liquid nitrogen cryostat setup described in Ref. 24 with a thermal gradient of 2°C at each average temperature point. The thermopower as a function of average temperature are shown in Fig. 2. The undoped films had a negative thermopower, indicating electrons as the majority carrier in the material. Upon incorporation of 1 at% Mg, the thermopower sign inverted to a positive value of ~187 μV/K indicating holes as the majority carrier, confirming that Mg was behaving as an acceptor. The decrease in the magnitude of the thermopower to ~88 μV/K with increased magnesium content indicates a movement of the Fermi level (E_f) towards the valence band, which would result in a higher hole concentration in the valence band. This result agrees with the $\sigma(T)$ shown in Fig. 1.

In addition to demonstrating the *p*-type doping, we also doped the material *n*-type. The group VI element tellurium was used to dope the material *n*-type. Tellurium doping was achieved by heating a PbTe source during growth. The PbTe decomposes on the substrate at the growth temperature resulting in the uniform incorporation of Te and rejection of Pb. RBS measurements confirm that no Pb is present and only Te atoms are incorporated in the film. For a Te concentration of 0.25 at% the conductivity increased to 0.25 S/cm and the thermopower remained negative while decreasing in magnitude to -

180 μV/K. Again, the decrease in magnitude indicates a shift of E_f, but this time the shift is towards the conduction band for a higher free electron concentration.

In order to achieve the doping of $GaN_{1-x}As_x$ in the intermediate composition range, the gallium BEP was increased above typical values for the deposition of uniform homogeneously amorphous material. This results in a driving force for the formation of crystalline GaAs:N (c-GaAs:N) clusters; this can be observed in the x-ray diffraction (XRD) and transmission electron microscopy (TEM) shown in Fig. 3. The dashed line XRD pattern in Fig. 3(a) is from a representative $GaN_{0.35}As_{0.65}$:Mg sample grown on a sapphire substrate with electrical properties described in Figs. 1 and 2. From the c-GaAs:N (111) XRD peak shift, the N incorporation fraction in the c-GaAs:N is estimated to be 7-8 mol%. The low magnification Z-contrast TEM image (TEAM 0.5 – 300 keV) shown in Fig. 3(b) reveals the distribution of the two phases: As-rich polycrystalline GaAs:N (bright), and intermediate As content amorphous $GaN_{1-x}As_x$ with a low density of nanocrystallites (dark). The two phases contribute to the average nominal composition of $GaN_{0.35}As_{0.65}$ determined by RBS. The density of the respective phases is not dependent on the Mg concentration, but instead is a result of the higher Ga BEP. The rings with spots (1, 2 and 3) indexed in the selected area diffraction pattern (JEOL 3010 – 300 keV) in Fig. 3(c) correspond to c-GaAs:N. They are superimposed on two broad rings (marked by black arrows) that are typical for amorphous material. The high-resolution TEM images (JEOL CM300 – 300 keV) in Fig. 3(d) & (e) show the amorphous regions (dark contrast in Fig. 3(b)) and polycrystalline grains (bright contrast in Fig. 3(b)) respectively. By adjusting the growth conditions, the relative intensity of the c-GaAs:N XRD peak intensity can be reduced, as seen in the solid line of Fig. 3(a). For

this sample, the As flux was reduced from 5.5×10^{-6} to 2.0×10^{-6} Torr in order to minimize the formation of c-GaAs:N while maintaining a relatively high conductivity of 0.17 S/cm. Due to the higher Ga BEP, these $GaN_{1-x}As_x$ alloys are mixed phase with polycrystalline GaAs:N phase present in an amorphous $GaN_{1-x}As_x$ matrix.

Despite the crystallinity in the samples for which electrical data is presented, the c-GaAs:N phase are embedded in an amorphous $GaN_{1-x}As_x$ matrix and we cannot yet determine which phase dominates the electrical properties. However, if the amorphous phase were highly insulating, the hopping between conductive c-GaAs:N would not result in the high conductivities and low conduction E_a observed.

IV. CONCLUSIONS

In conclusion, we have demonstrated control over the electrical properties of mixed phase $GaN_{1-x}As_x$. Both *p*-type and *n*-type doping was achieved as confirmed by conductivity and thermopower measurements. The wide range of band gaps accessible using this material makes it promising for solar conversion devices. Our work opens opportunities for possibly functionalizing this material and other amorphous III-V alloys, as well as the fundamental study of defect physics in amorphous III-V semiconductors.

ACKNOWLEDGEMENTS

This work was supported by the Director, Office of Science, Office of Basic Energy Sciences, Materials Sciences and Engineering Division, of the U.S. DOE under

Contract No. DE-AC02-05CH11231. O.D.D. acknowledges support from National Science Foundation Contract No. DMR-0349257. The use of the National Center for Electron Microscopy at Lawrence Berkeley Laboratory is appreciated. The growth work at the University of Nottingham was supported by the EPSRC (Grant Nos. EP/I004203/1, EP/G046867/1 and EP/G030634/1). A.X.L. acknowledges the National Science Foundation for financial support

References

[1] W. E. Spear, *Adv. in Phys.* **26** 811 (1977).

[2] W. E. Spear, P. G. Le Comber, S. Kinmond, and M. H. Brodsky, *Appl. Phys. Lett.* **28**, 105 (1976).

[3] D. E. Carlson and C. R. Wronski, *Appl. Phys. Lett.* **28**, 671 (1976).

[4] J. Yang, A. Banerjee, and S. Guha, *Appl. Phys. Lett.* **70,** 2975 (1997).

[5] Y. Tawada, H. Okamoto, and Y. Hamakawa, *Appl. Phys. Lett.* **39**, 237 (1981).

[6] W. H. Paul, J. H. Chen, E. Z. Liu, A. E. Wetsel, and P. Wickboldt, **164,** 1-10 (1993).

[7] A. Morimoto, T. Miura, M. Kumeda, and T. Shimizu, *J. Appl. Phys.* **53** 7299 (1982).

[8] H. Hargreaves, M. J. Thompson, and D. Turner, *J. Non-Cryst. Sol.* **35-36,** 403 (1980).

[9] Y. Segui, F. Carrere, and A. Bui, *Thin Solid Films* **92** 303 (1982).

[10] R. A. Street and K. Winer, *Phys. Rev. B* **40**, 6236 (1989).

[11] J. Robertson, *Phys. Rev. B* **33**, 4399 (1986).

[12] J. Kakalios, R. A. Street, *Phys. Rev. B* **34**, 6014 (1986).

[13] W. Walukiewicz, W. Shan, K. M. Yu, J. W. Ager III, E. E. Haller, I. Miotkowski, M. J. Seong, H. Alawadhi, and A. K. Ramdas, *Phys. Rev. Lett.* **85**, 1552 (2000).

[14] W. Shan, W. Walukiewicz, J. W. Ager III, E. E. Haller, J. F. Geisz, D. J. Friedman, J. M. Olson, and S. R. Kurtz, *Phys. Rev. Lett.* **82**, 1221 (1999).

[15] K. Uesugi, N. Morooka, and I. Suemune, *Appl. Phys. Lett.* **74**, 1254 (1999).

[16] J. Wu, W. Walukiewicz, K. M. Yu, J. D. Denlinger, W. Shan, J. W. Ager III, A. Kimura, H. F. Tang, and T. F. Kuech, *Phys. Rev. B* **70**, 115214 (2004).

[17] S. V. Novikov, C. R. Staddon, A. V. Akimov, R. P. Campion, N. Zainal, A. J. Kent, C. T. Foxon, C. H. Chen, K. M. Yu, and W. Walukiewicz, *J. Cryst. Growth* **311,** 3417–3422 (2009).

[18] K. M. Yu, S. V. Novikov, R. Broesler, I. N. Demchenko, J. D. Denlinger, Z. Liliental-Weber, F. Luckert, R. W. Martin, W. Walukiewicz, and C. T. Foxon, *J. Appl. Phys.* **106**, 103709 (2009).

[19] K. M. Yu, S. V. Novikov, R. Broesler, Z. Liliental-Weber, A. X. Levander, V. M. Kao, O. D. Dubon, J. Wu, W. Walukiewicz, and C. T. Foxon, *Appl. Phys. Lett.* **97**, 101906 (2010).

[20] P. Stumm and D. A. Drabold, *Phys. Rev. Lett.* **79**, 677 (1997).

[21] A. X. Levander, Z. Liliental-Weber, R. Broesler, M. E. Hawkridge, S. V. Novikov, C. T. Foxon, O. D. Dubon, J. Wu, W. Walukiewicz, and K. M. Yu, *Appl. Phys. Lett.* **98**, 161902 (2011).

[22] F. Mireles and S. E. Ulloa, *Phys. Rev. B* **58**, 3879 (1998).

[23] M. Stutzmann, D. K. Biegelsen, and R. A. Street, *Phys. Rev. B.* **35**, 5666 (1987).

[24] J. W. Ager III, *Phys. Stat. Sol. (b).* **245**, 873 (2008).

Figure Captions

Fig. 1. Conductivity as a function of temperature for $GaN_{0.35}As_{0.65}$:Mg samples with varying Mg content given in atomic percents. The inset table gives activation energies calculated from the linear low temperature region of the curve to the right side of the dashed line (50-6K).

Fig. 2. Thermopower as a function for temperature for $GaN_{0.35}As_{0.65}$:Mg samples with varying Mg content (same samples as shown in Fig. 1). The positive sign for Mg doped samples shows Mg behaving as an acceptor. The error bars signify the standard deviation from three measurements at a given average temperature. Higher resistance samples have larger errors due to the uncertainties in measuring small voltages across large resistances.

Fig. 3. Structural analysis of $GaN_{0.35}As_{0.65}$:Mg samples. Representative x-ray diffraction pattern of samples discussed in Figs. 1 & 2 (dashed) and sample grown under lower As BEP to reduce crystallinity (solid) (a). Low magnification Z-contrast transmission electron microscopy image, selected area diffraction, and high-resolution TEM images of a sample discussed in Figs. 1 & 2 (b), (c), (d), and (e) respectively. In (b), the bright contrast is the c-GaAs:N phase shown in (e) and the dark contrast is the amorphous $GaN_{1-x}As_x$ phase shown in (d). The diffraction pattern (c) shows a superposition of c-GaAs:N rings from (111), (220), and (311) planes indicated by 1, 2, and 3 and two broad amorphous rings indicated by arrows.

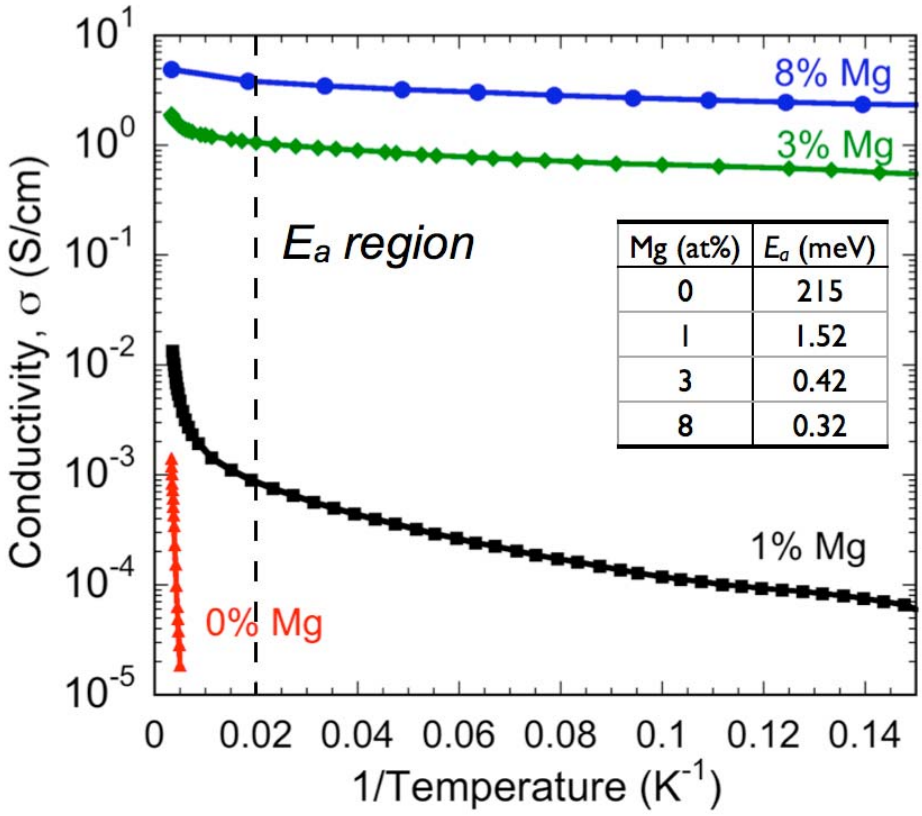
Conductivity, σ (S/cm)
1/Temperature (K^{-1})
8% Mg
3% Mg
1% Mg
0% Mg
E_a region
Mg (at%) | E_a (meV)
0 | 215
1 | 1.52
3 | 0.42
8 | 0.32

Fig. 1.

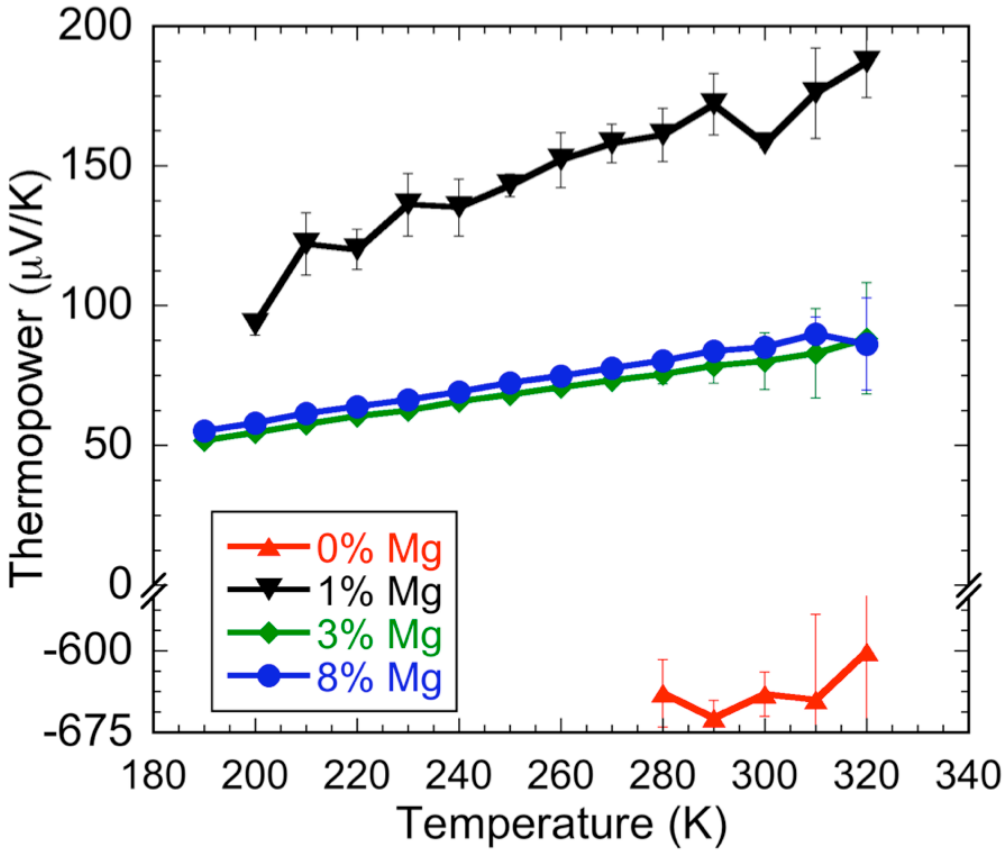
Thermopower (μV/K)
Temperature (K)
0% Mg
1% Mg
3% Mg
8% Mg
200
150
100
50
0
-600
-675
180
200
220
240
260
280
300
320
340

Fig. 2.

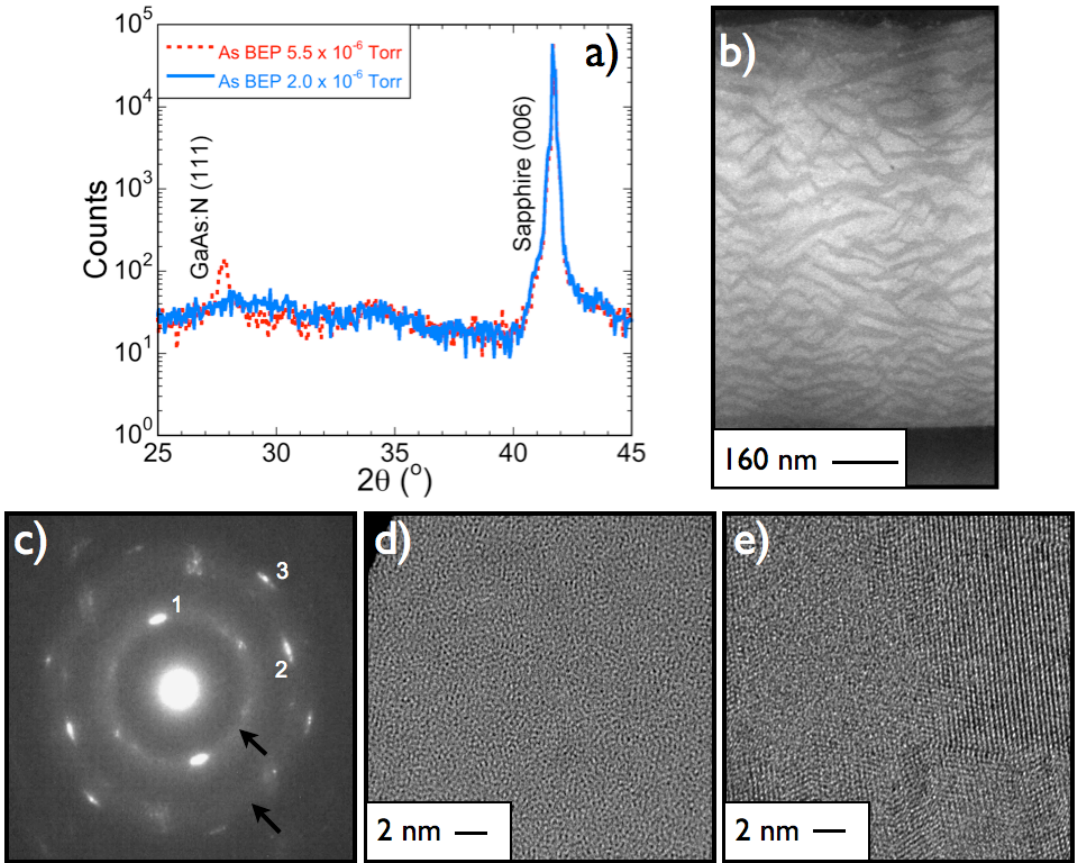
a)
As BEP 5.5 x 10^-6 Torr
As BEP 2.0 x 10^-6 Torr
GaAs:N (111)
Sapphire (006)
Counts
2θ (°)
b)
160 nm
c)
1
2
3
d)
2 nm
e)
2 nm

Fig. 3.

DISCLAIMER

This document was prepared as an account of work sponsored by the United States Government. While this document is believed to contain correct information, neither the United States Government nor any agency thereof, nor The Regents of the University of California, nor any of their employees, makes any warranty, express or implied, or assumes any legal responsibility for the accuracy, completeness, or usefulness of any information, apparatus, product, or process disclosed, or represents that its use would not infringe privately owned rights. Reference herein to any specific commercial product, process, or service by its trade name, trademark, manufacturer, or otherwise, does not necessarily constitute or imply its endorsement, recommendation, or favoring by the United States Government or any agency thereof, or The Regents of the University of California. The views and opinions of authors expressed herein do not necessarily state or reflect those of the United States Government or any agency thereof or The Regents of the University of California.